Graphene Fiber-based Asymmetric Micro-supercapacitors

Department of Polymer Science and Engineering, Zhejiang University

*Bingna Zheng (11029021), Chao Gao**

Introduction

Fiber-based micro-supercapacitors (F-mSCs) are new members of the energy storage family, which facilitate SCs with flexibility and expand their application to fields such as tiny, flexible and wearable devices. One of the biggest challenges for F-SCs is to enhance the energy density (*E*) and keep the flexibility at the same time.

Here, for the first time we assembled a kind of fiber-based asymmetric micro-supercapacitors (F-*asym*-mSCs) with two different graphene fiber-based electrodes. The excellent electrochemical performances (59.2 mF/cm^2 and 32.6 mF/cm^2, respectively) of both electrodes offered a chance to achieve high performance two-ply F-*asym*-mSCs. The potential window of F-*asym*-mSCs was expanded to 1.6 V, and both of the area energy density (E_A , 11.9 μWh/cm^2) and volume energy density (E_V, 11.9 mWh/cm^3) are the highest *E* ever reported in F-SCs. The F-*asym*-mSCs exhibit good cycling stability with a 92.7% initial capacitance retention after 8000 cycles and can be integrate into a fiber-like device to realize the flexibility of fibers.

Negative Electrode

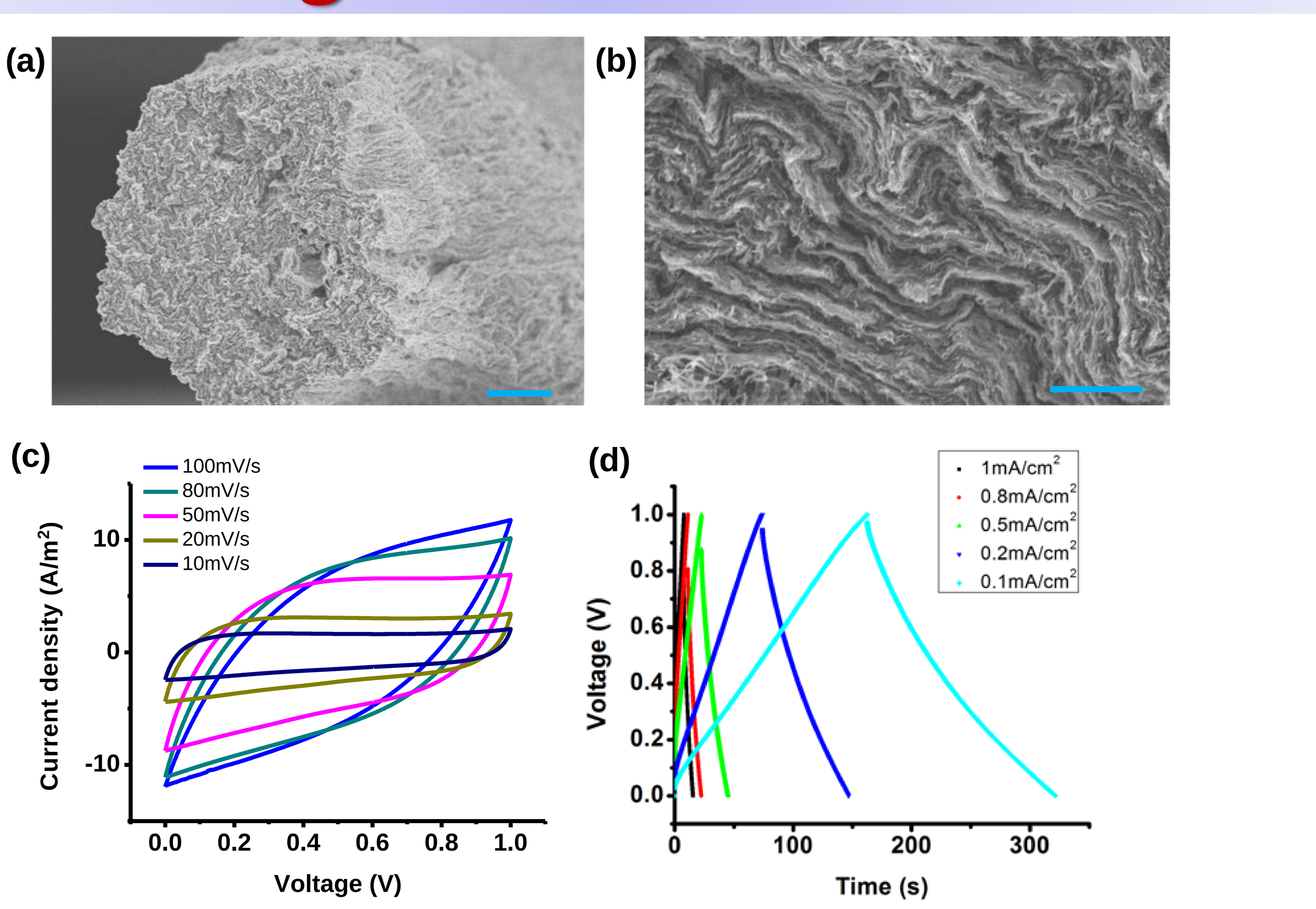

Figure 4. (a) and (b) Cross-section images of GCF observed by SEM, scale bars: 5μm and 1μm . (c) CV curves of GCF at different scan rates. (d) GCD curves at different current densities.

Asymmetric Supercapacitor

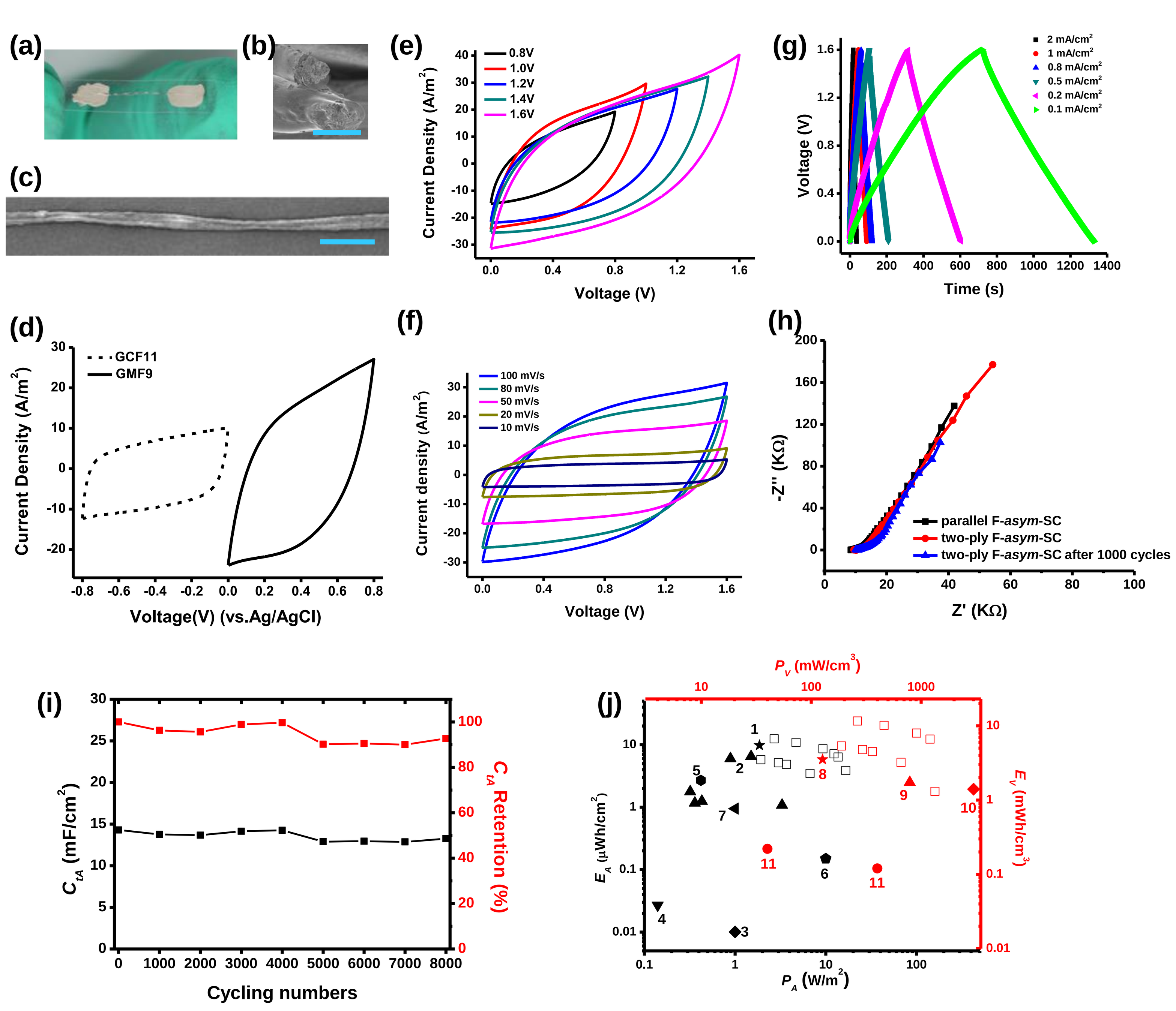

Figure 5. (a) Photograph of two-ply F-*asym*-mSC. (b) Cross-section image of two-ply F-*asym*-mSC observed by SEM, scale bar: 50 μm. (c) Surface image of two-ply F-*asym*-mSC observed by SEM, scale bar: 200 μm. (d) CV curves of GMF and GCF in three-electrode system (vs. Ag/AgCl). (e) CV curves of parallel F-*asym*-mSCs at different potential windows (scanning rate 100 mV/s). (f) CV curves of two-ply F-*asym*-mSC at different scanning rates when operating voltage is 1.6 V. (g) GCD curves of two-ply F-*asym*-mSC at different current densities when operating voltage is 1.6 V. (h) Nyquist plots of F-*asym*-mSCs.(i) Cycling performance of two-ply F-*asym*-mSCs tested by GCD at 1.0 mA/cm^2. (j) E_A-P_A and E_V-P_V plots of F-*asym*-mSCs and data from references, where the black symbols are calculated by area and red symbols are calculated by volume, square symbols are data of this work.

Positive Electrode

•Morphology

Reactions between Mn^{2+}, carbon and $KMnO_4$ led to the formation of MnO_2 :

$$2MnO_4^- + 3Mn^{2+} + 2H_2O —— 5MnO_2 + 4H^+$$

$$4MnO_4^- + 3C + H_2O —— 4MnO_2 + CO_3^{2-} + 2HCO_3^-$$

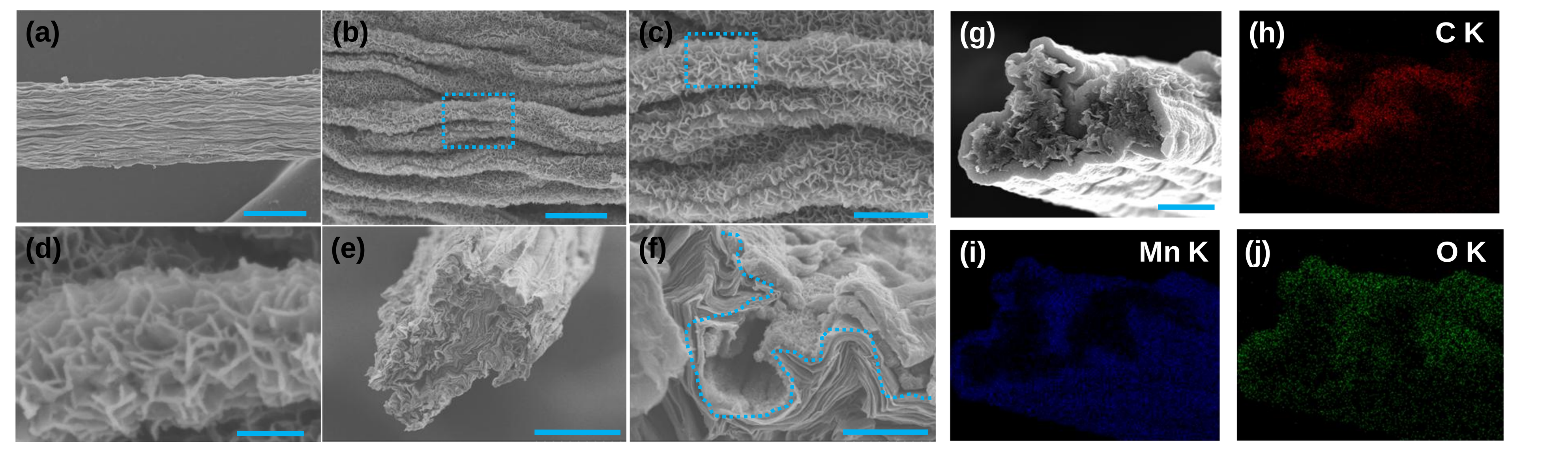

Figure 1. (a) - (d) Surface morphology of GMF1 observed by SEM, scale bar: 10 μm, 1 μm, 500 nm, and 150 nm. (e) and (f) Cross-section images of GMF1 observed by SEM, scale bar: 10 μm and 1 μm. (g) - (j) Elemental mapping images of GMF24 by EDAX, scale bar: 10 μm

•Characterization

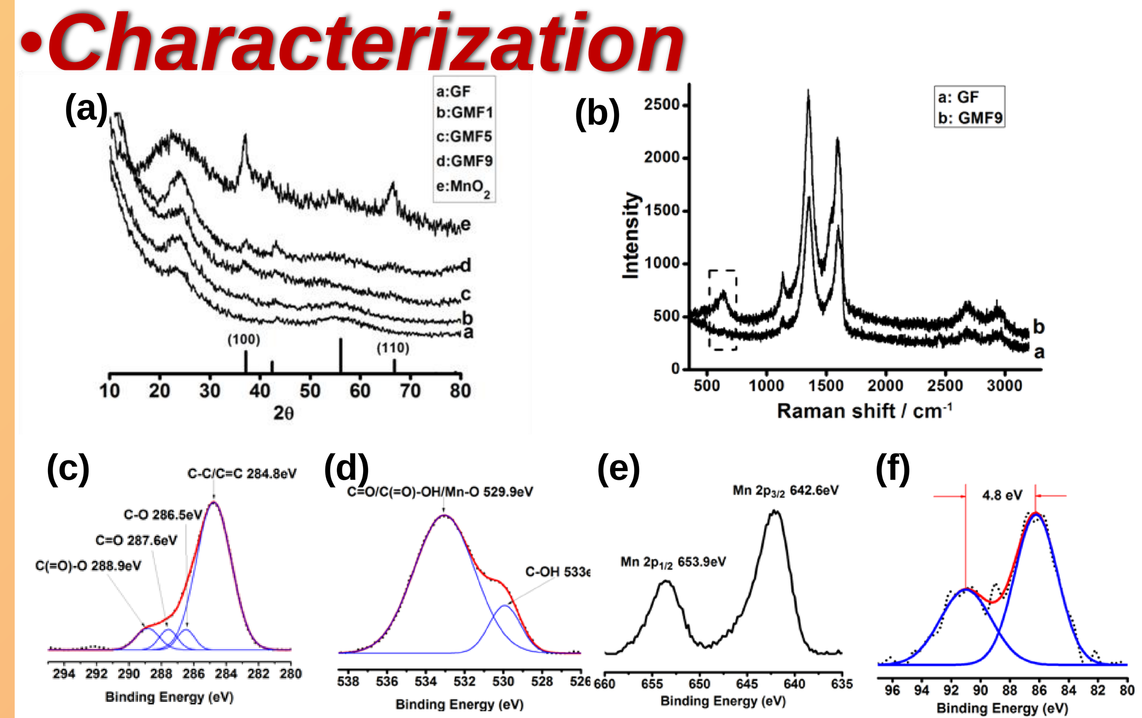

Figure 2. (a) XRD spectra of neat GF, GMF1, GMF5, GMF9, and MnO_2 comparing with standard XRD peak of ε-MnO_2. (b) Raman spectra of neat GF and GMF9. (c), (d), (e) and (f) C_{1s}, O_{1s}, Mn_{2p} and Mn_{3s} peaks in XPS of GMF, respectively.

•Electrochemistry

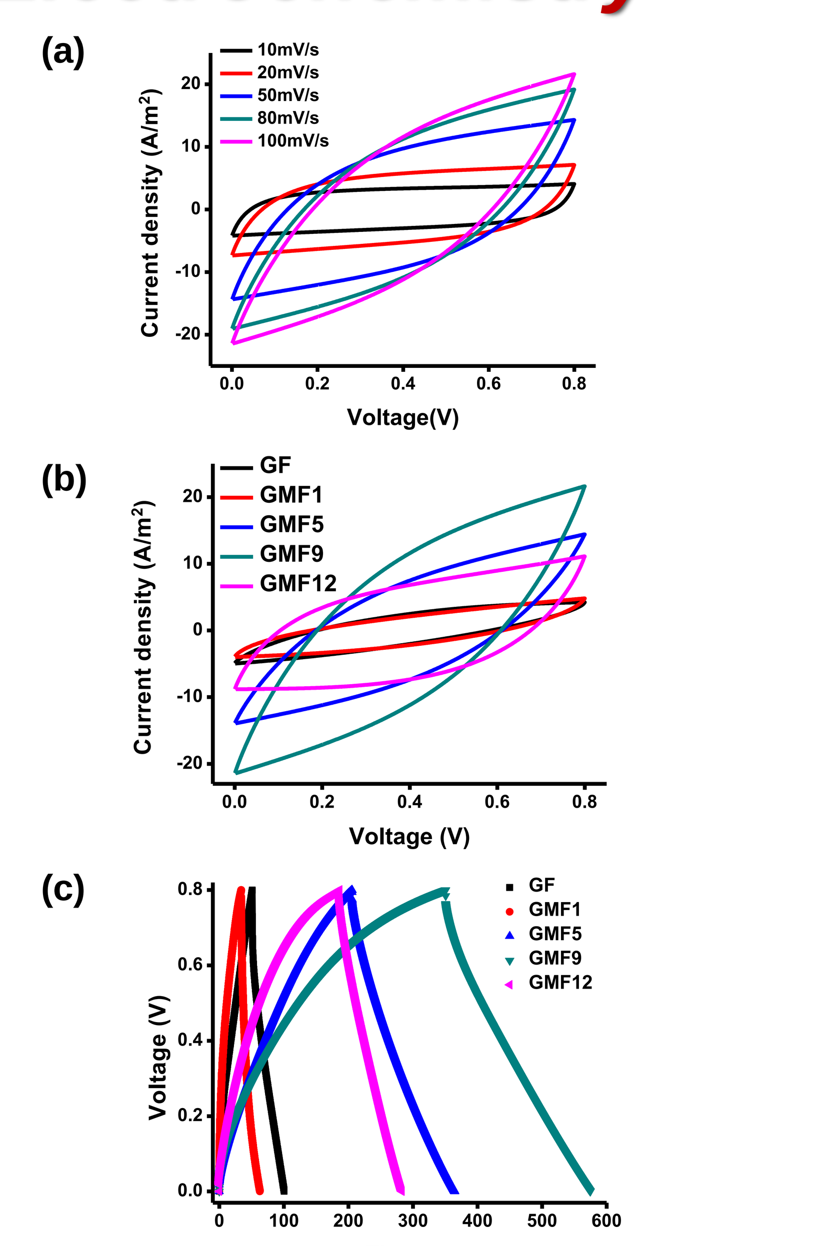

Figure 3. (a) CV curves of GMF9 at different scan rates, inset: cartoon illustration of F-mSC. (b) CV curves of neat GF, GMF1, GMF5, GMF9, and GMF12 at 100 mV/s. (c) GCD curves of neat GF, GMF1, GMF5, GMF9, and GMF12 at current density of 0.1 mA/cm^2.

Scheme

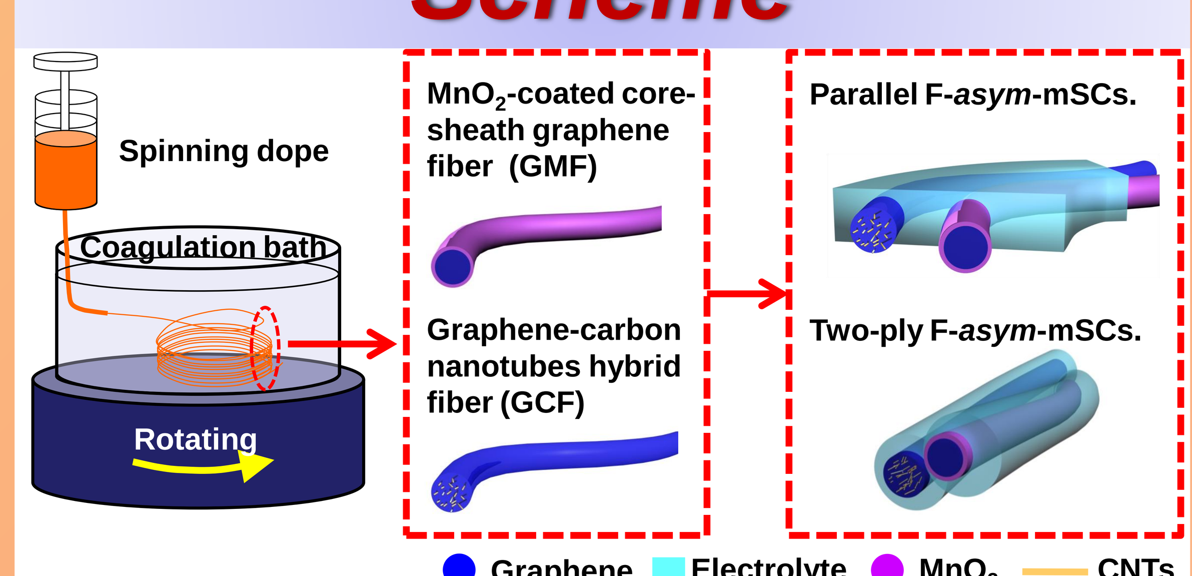

Conclusions

We have prepared two different graphene-based fiber electrodes based on the facile wet-spinning assembly method. The core-sheath GMFs integrated the advantages of pseudo-capacitance of MnO_2 and conductivity of graphene. The synergistic effect of graphene and CNTs enhanced C_A of GCFs. For the first time, we fabricated F-*asym*-mSCs from the excellent GMF and GCF electrodes. Due to the large voltage window, the energy densities of flexible F-*asym*-mSCs were significantly improved to 11.9 μWh/cm^2, the highest values ever reported for all F-SCs. The F-*asym*-mSCs exhibit good cycling stability with a 96.3% initial capacitance retention after 1000 cycles.

Acknowledgements

This work is funded by the National Natural Science Foundation of China (no. 21325417 and no. 51173162), Huawei Innovation Research Program, Fundamental Research Funds for the Central Universities (no. 2013XZZX003), and Zhejiang Provincial Natural Science Foundation of China (no. R4110175).

References

1. V. T. Le, H. Kim. A. Ghosh, J. Kim, J. Chang, Q. A. Vu, D. T. Pham, J. Lee, S. Kim, Y. H. Lee, *ACS Nano*, 2013, 7, 5940.
2. J. Ren, W. Bai, G. Guan, Y. Zhang, H. Peng, *Adv. Mater.*, 2013, 25, 5965.
3. Y. Meng, Y. Zhao, C. Hu, H. Cheng, Y. Hu, Z. Zhang, G. Shi, L. Qu, *Adv. Mater.*, 2013, 25, 2326.
4. J. Bae, M. K. Song, Y. J. Park, J. M. Kim, M. Liu, Z. L. Wang, *Angew. Chem. Int. Ed.*, 2011, 50, 1683.
5. Y. Fu, X. Cai, H. Wu, Z. Lv, S. Hou, M. Peng, X. Yu, D. Zou, *Adv. Mater.*, 2012, 24, 5713.
6. T. Chen, L. Qiu, Z. Yang, Z. Cai, J. Ren, H. Li, H. Lin, X. Sun, H. Peng, *Angew. Chem. Int. Ed.*, 2012, 41, 11977.
7. Y. Fu, H. Wu, S. Ye, X. Cai, X. Yu, S. Hou, H. Kafafy, D. Zou, *Energy Environ. Sci.*, 2013, 6, 805.
8. C. Choi, J. A. Lee, A. Y. Choi, Y. T. Kim, X. Lepró, M. D. Lima, R. H. Baughman, S. J. Kim, *Adv. Mater.*, 2013, DOI: 10. 1002/ adma. 201304736.
9. J. Ren, L. Li, C. Chen, X. Chen, Z. Cai, L. Qiu, Y. Wang, X. Zhu, H. Peng, *Adv. Mater.*, 2013, 25, 1155.
10. J. A. Lee, M. K. Shin, S. H. Kim, H. U. Cho, G. M Spinks, G. G. Wallace, M. D. Lima, X. Lepró, M. E. Kozlov, R. H. Baughman, S. J. Kim, *Nat Commun*, 2013, 4, 1970.
11. X. Xiao, T. Li, P. Yang, Y. Gao, H. Jin, W. Ni, W. Zhan, X. Zhang, Y. Cao, J. Zhong, L. Gong, W. Yen, W. Mai, J. Chen, K. Huo, Y. Chueh, Z. L. Wang, J. Zhou, *ACS Nano*, 2012, 6, 9200.